Frequency characteristics of the response of water pressure in a closed well to volumetric strain in the high-frequency domain

Yuichi Kitagawa,[1] Satoshi Itaba,[1] Norio Matsumoto,[1] and Naoji Koizumi[1]

Received 18 June 2010; revised 28 April 2011; accepted 5 May 2011; published 3 August 2011.

[1] Oscillations of water pressures and crustal strains due to the seismic waves of the 2010 Chile earthquake were observed in Japan. The oscillations of water pressures observed over the frequency range of 0.002 to 0.1 Hz were negative proportional to the oscillations of volumetric strains. The responses of water pressures in closed wells are frequency-dependent. The expression for the response of water pressure in a closed well to crustal strain is developed based on the poroelastic theory. The expression developed in the present paper describes the frequency characteristics of the responses. The response is useful for the estimation of rock properties. In addition, the responses of water pressure due to tidal volumetric strain are estimated and compared with the responses due to the seismic waves.

Citation: Kitagawa, Y., S. Itaba, N. Matsumoto, and N. Koizumi (2011), Frequency characteristics of the response of water pressure in a closed well to volumetric strain in the high-frequency domain, *J. Geophys. Res.*, *116*, B08301, doi:10.1029/2010JB007794.

1. Introduction

[2] Water level oscillations in open wells have been reported to be caused by seismic waves. *Cooper et al.* [1965] and *Liu et al.* [1989] formulated analytical solutions of water level oscillations in open wells due to seismic waves and successfully described the characteristics of the responses of water levels, such as the amplification of the response due to resonance and the attenuation of the response in the high-frequency range. The frequency characteristics of the responses of water levels in open wells to cyclic loadings, such as earth tides and barometric pressure, were formulated by *Hsieh et al.* [1987] and *Rojstaczer* [1988], among others. These formulations also indicate that the response decays in the high-frequency range. The attenuation in the high-frequency range is an effect of wellbore storage. Thus, both theory and observation indicate that the amplitude of the response in an open well is smaller and that the phase lag increases as the frequency increases.

[3] Previously, based on the poroelastic theory, the response of water pressure in a closed well in the high-frequency range was thought to be the same as the undrained response of pore water pressure in rock. The poroelastic theory describes the coupled theory between deformation of poroelastic rock and pore water flow. *Roeloffs* [1996] and *Wang* [2000] comprehensively reviewed a number of studies related to the poroelastic theory. Under assumption of an undrained condition, i.e., under the condition that there is no flow of pore water, the poroelastic theory indicates that the pore water pressure change is simply proportional to the mean stress change and the volumetric strain change of the rock. Stated differently, the response of pore water pressure to the change in stress or strain is constant with no phase lag.

[4] *Kano and Yanagidani* [2006] compared water pressure oscillations in closed wells with the ground velocity of the broadband seismometer due to teleseismic waves and showed that the frequency response of water pressure to the radial component of the ground motion below 2 Hz is flat. In contrast, *Kitagawa et al.* [2006] calculated the response of water pressure in a closed well to strain due to the seismic waves of the 2004 Sumatra-Andaman earthquake and estimated that the response became smaller with increasing frequency. However, even the water pressure change in a closed well requires a small amount of water flow between the aquifer and the well. Thus, the response of water pressure in a closed well is predicted to be frequency-dependent.

[5] Oscillations of water pressures and crustal strains due to the seismic waves of the 2010 Chile earthquake were observed in Japan. In this work, the oscillations of water pressures in closed wells due to the seismic waves of the earthquake are compared with the oscillations of crustal strain. The frequency characteristics of the responses of water pressure in closed wells to volumetric strains are estimated. The response of water pressure in a closed well to cyclic volumetric strain is formulated based on the quasi-static poroelastic theory, in reference to the derivation scheme for the response of water level of an open well reported by *Hsieh et al.* [1987]. The expression developed in the present paper is compared with the responses estimated

[1]Active Fault and Earthquake Research Center, Geological Survey of Japan, National Institute of Advanced Industrial Science and Technology, Tsukuba, Japan.

0148-0227/11/2010JB007794

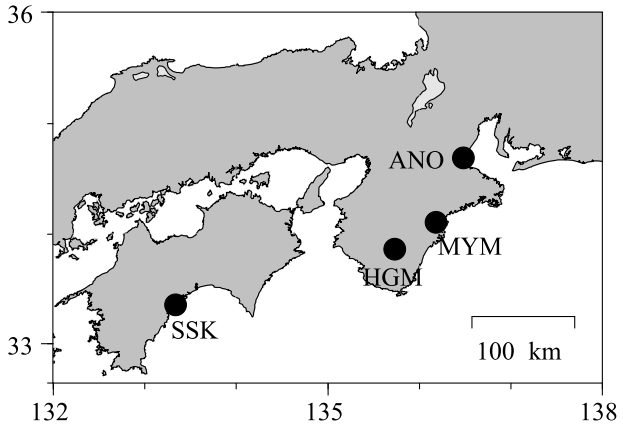

Figure 1. Map of the four stations.

from observed data. In addition, the responses of water pressures due to tidal volumetric strain are estimated and compared with the responses due to the seismic waves.

2. Observations

2.1. Outline of Measurement

[6] The Active Fault and Earthquake Research Center, the Geological Survey of Japan, AIST, has a network composed of approximately 50 groundwater observation stations in and around the Tokai, Kinki, and Shikoku regions in Japan. At these stations, groundwater levels are continuously monitored. At about half of the stations, crustal strains are also monitored with borehole strainmeters. Data have typically been recorded at a sampling rate of 2 min. However, at stations that have been constructed since 2006, data are recorded at sampling rates of 1 s or higher in order to observe the oscillation due to seismic wave.

[7] In the present paper, water pressures in five closed wells at four stations (Figure 1 and Table 1) are examined. These wells satisfy the following requirements. First, the well is an artesian well and is closed by bolting using a sealed iron cover and hard rubber packing on the head of the well casing. The sensor cables are fixed by bolting using hard rubber packing. Second, the water pressure data for the closed well are recorded at a sampling rate of 1 s or higher. Third, the horizontal and vertical crustal strains are observed at the same station and are recorded at a sampling rate of 1 s or higher (Table 2). The water pressures in the five closed wells are observed using Digiquartz® sensors (Model 8WD or Series 6000 of Paroscientific, Inc.). The water pressure data are converted into the units used to measure the water level, i.e., meters. The crustal strains at the four stations are observed using Ishii-type borehole strainmeters [*Ishii et al.*, 2002].

2.2. Geology and Hydrology of the Stations

[8] The ANO station is located on the Ryoke metamorphic belt. The rock consists of granitic rocks, in particular coarse-grained granodiorite. The boring cores and the borehole televiewer logging reveals that the dips of the fractures are primarily horizontal or at low angles. Based on the fluid electric conductivity (FEC) logging and the temperature logging, major permeable fractures are found at depths of 504 and 528 m for the ANO1 well and at depths of 105, 201, and 208 m for the ANO2 well.

[9] The HGM station is located on the Shimanto formation, which is the Nankai accretionary prism. The rock consists of alternating layers of sandstone and shale. In particular, the shale is schistose and wholly fragmented. From the borehole televiewer logging, the dips of the fractures vary over a wide angle. Based on the temperature logging of the HGM2 well, major groundwater discharges are found at depths of 78 and 190 m.

[10] The MYM station is located on the northern margin of the northern unit of the Kumano acidic rocks. The rock consists of granite porphyry. Based on the boring cores and the borehole televiewer logging, the dips of the fractures in the rock are primarily at high angles, which are larger than 70 degrees. Based on the FEC logging, major permeable fractures in the depth range of from 200 to 580 m are found at depths of 210, 285–295, 370–385, and 422 m for the MYM1 well.

[11] The SSK station is located on the northern Shimanto belt, which is the Nankai accretionary prism. The rock consists primarily of shale and some sandstone. Based on the borehole televiewer logging, the dips of the fractures vary over a wide angle. From the hydrophone VSP logging in the depth range of from 200 to 570 m at the SSK1 well, tube waves are found to exist at 13 depths (at intervals of several ten meters), and many open fractures are thought to exist. Based on the FEC logging in the depth range of from 200 to 570 m, major permeable fracture is estimated at a depth of 365 m for the SSK1 well.

3. Data Analysis

3.1. Oscillations Due to the Chile Earthquake

[12] On 27 February 2010, an earthquake (Mw 8.8) occurred in the Chile subduction zone [e.g., *Lay et al.*,

Table 1. Information of Five Closed Wells and Water Pressure Observations

Station Code	Well Code	Latitude (°N)	Longitude (°E)	Height Above the Sea Level (m)	Length of Well Casing (m)	Radius of Well Casing (m)	Radius of Drilling (m)	Depth of Screen (m)	Length of Screen (m)	Sampling Rate of Data (Hz)
ANO	ANO1	34.7869	136.4019	165	570	0.075	0.135	499.2 ~ 514.4	15	20
ANO	ANO2	34.7871	136.4017	166	240	0.075	0.135	195.6 ~ 209.1	14	20
HGM	HGM2	33.8674	135.7318	121	200	0.075	0.135	171.4 ~ 192.5	21	1
MYM	MYM1	34.1123	136.1815	29	580	0.075	0.135	375.2 ~ 435.0	60	1
SSK	SSK1	33.3896	133.3229	16	570	0.075	0.135	337.4 ~ 378.5	41	20

Table 2. Information of Strainmeters at the Four Stations

Station Code	Well Code	Latitude (°N)	Longitude (°E)	Height Above the Sea Level (m)	Depth of Strainmeter (m)	Sampling Rate of Data (Hz)	A_{vs} (dimensionless)
ANO	ANO1	34.7869	136.4019	165	588.9 ~ 590.3	20	1.8
HGM	HGM1	33.8675	135.7318	121	372.7 ~ 374.1	20	3.4
MYM	MYM1	34.1123	136.1815	29	590.0 ~ 591.4	20	3.4
SSK	SSK1	33.3896	133.3229	16	576.7 ~ 578.1	20	1.5

2010]. Oscillations of the crustal strains and water pressures associated with the seismic waves of the earthquake were observed at the stations of Geological Survey of Japan. Figure 2 shows the data for the crustal strains at ANO1 and the water pressures at ANO1 and ANO2. The water pressure changes are negative proportional to strain in the radial direction and volumetric strain and are proportional to vertical strain. Figure 3 shows the Fourier amplitude of the volumetric strain at ANO1 and the water pressure at ANO1. The range of frequencies of the seismic waves is from 0.002 to 0.1 Hz, concentrated in the ranges 0.004 to 0.006 Hz and 0.03 to 0.06 Hz. The signal around 0.2 Hz indicates a microtremor.

3.2. Estimation of Amplification Factor of Crustal Strain by Borehole Strainmeter

[13] The structure around the borehole strainmeter amplifies the crustal strain. In general, the strain data observed by the borehole strainmeter are larger than the actual crustal strains. A few methods for the correction of amplification have been proposed. In the present paper, the amplification factor is calculated using synthetic seismograms of strain calculated from the source solution of the earthquake as the real crustal strain. The amplification factor A_{vs} for volumetric strain is expressed as

$$A_{vs} = \frac{\varepsilon_{kk}^{obs}}{\varepsilon_{kk}}, \tag{1}$$

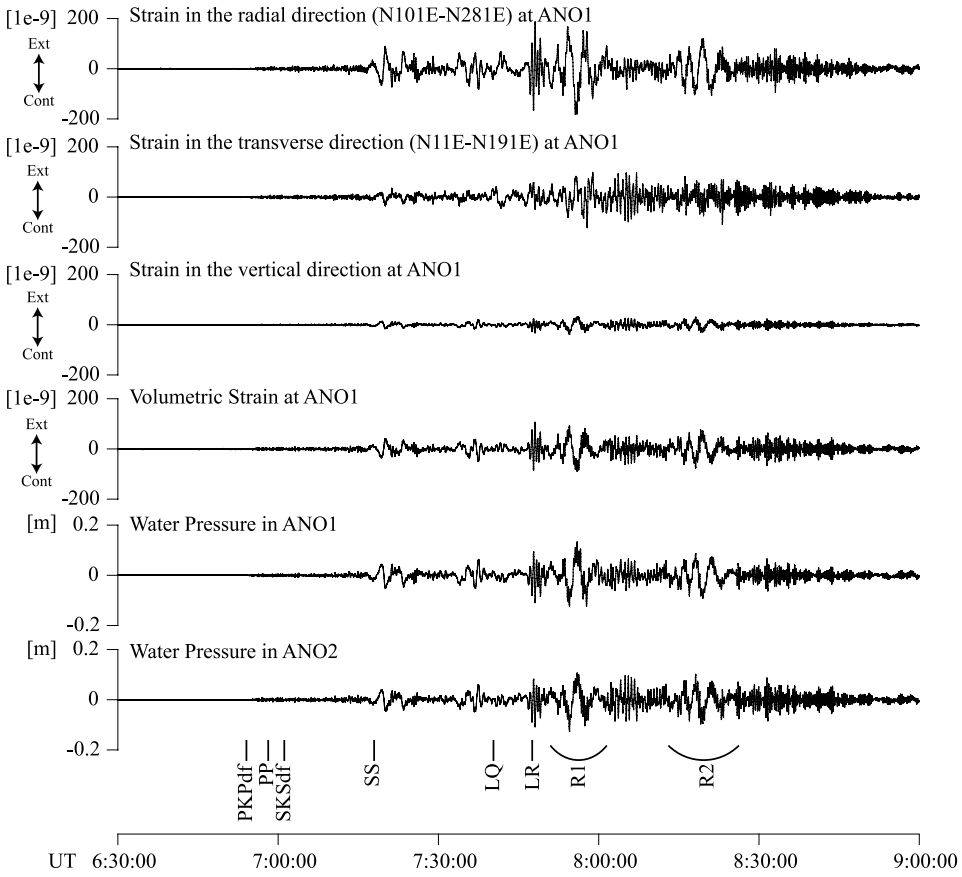

Figure 2. Observation results of crustal strains at ANO1 and water pressures at ANO1 and ANO2 on 27 February 2010. The graphs show the traces produced by applying a band-pass Butterworth filter from 0.002 to 0.1 Hz to raw data. The travel time of the phases of the seismic waves are estimated from the Website of USGS (http://neic.usgs.gov/neis/travel_times/compute_tt.html) and the Website of ERI, University of Tokyo (http://outreach.eri.u-tokyo.ac.jp/2010/03/201003_centralchile/).

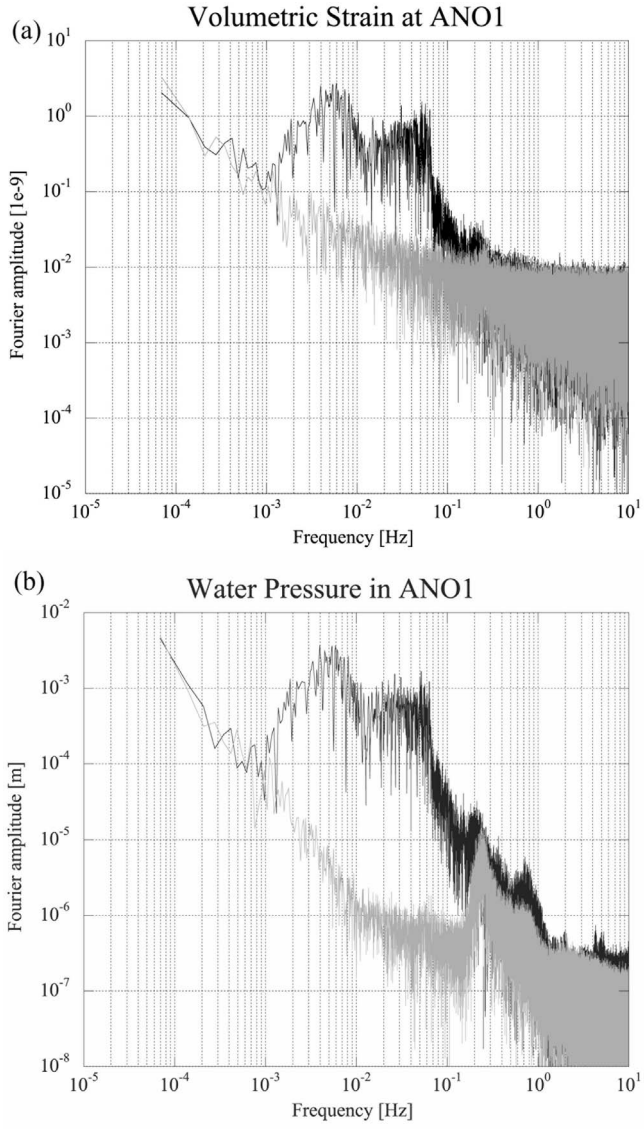

Figure 3. Amplitude spectra of (a) volumetric strain at ANO1 and (b) water pressure at ANO1. The black lines indicate the spectra for the data from 27 February 2010, 06:00:00 to 10:00:00 (UT) for the 2010 Chile earthquake, and the gray lines indicate the spectra for the data from 26 February 2010, 06:00:00 to 10:00:00 (UT) for noise levels.

where ε_{kk}^{obs} is the volumetric strain data obtained from the borehole strainmeter, and ε_{kk} is the real volumetric strain. The real volumetric strain ε_{kk} is calculated by summing all characteristic modes [*Dziewonski et al.*, 1981] using the global CMT solution of the 2010 Chile earthquake (http://www.globalcmt.org/). For the period range of from 333 to 500 s (0.002 to 0.003 Hz), which is much longer than the rupture duration (100 to 200 s) of the earthquake, the volumetric strain data obtained by the borehole strainmeter is compared with the synthetic seismograms of volumetric strain (Figure 4), and the amplification factor A_{vs} is estimated (Table 2).

3.3. Estimation of the Response Due to Seismic Waves

[14] For the water pressures in the five wells, the response to the volumetric strain at each station was calculated. In the following analysis, the data with a sampling rate of 20 Hz were resampled at 1 Hz without averaging. Figure 5 shows the amplitudes and the phase shifts of the responses using the data from 27 February 2010, 06:30:00 to 08:59:59 (UT). The phase shifts, including the time difference between the time stamp of the data and the actual time of A/D conversion of each device, are calculated. The responses at ANO1, HGM2, MYM1, and SSK1 are characterized by small amplitude and phase lag in the high-frequency side. The response at ANO2 has a constant amplitude and a slight phase lag in the range of from 0.002 to 0.1 Hz.

4. Theory

4.1. Formulation of Water Pressure Response in a Closed Well to Volumetric Strain

[15] Figure 6 shows a closed well-aquifer system. The well is an artesian well and is closed near the ground surface. The well is assumed to penetrate the entire thickness of the aquifer. The aquifer is assumed to be perfectly confined, isotropic, and homogeneous, and to extend laterally to infinity. The length and radius of the well casing are denoted by L_c and r_c, respectively. The length and radius of the screened portion of the well are denoted by L_s and r_s, respectively. The volume V_w of water in the well is expressed as

$$V_w = \pi r_c^2 (L_c - L_s) + \pi r_s^2 L_s. \tag{2}$$

Strain affects the water pressure in the well in two ways. One is the elastic deformation of water due to volume change of the well. The other is the water flow due to the difference between the pore water pressure in the aquifer

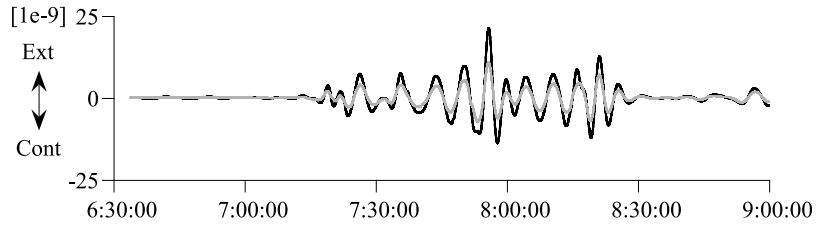

Figure 4. Volumetric strains at ANO1. The solid trace indicates the observation data, and the gray trace indicates the synthetic seismogram. The graph shows the traces obtained by applying a band-pass Butterworth filter from 0.002 to 0.003 Hz.

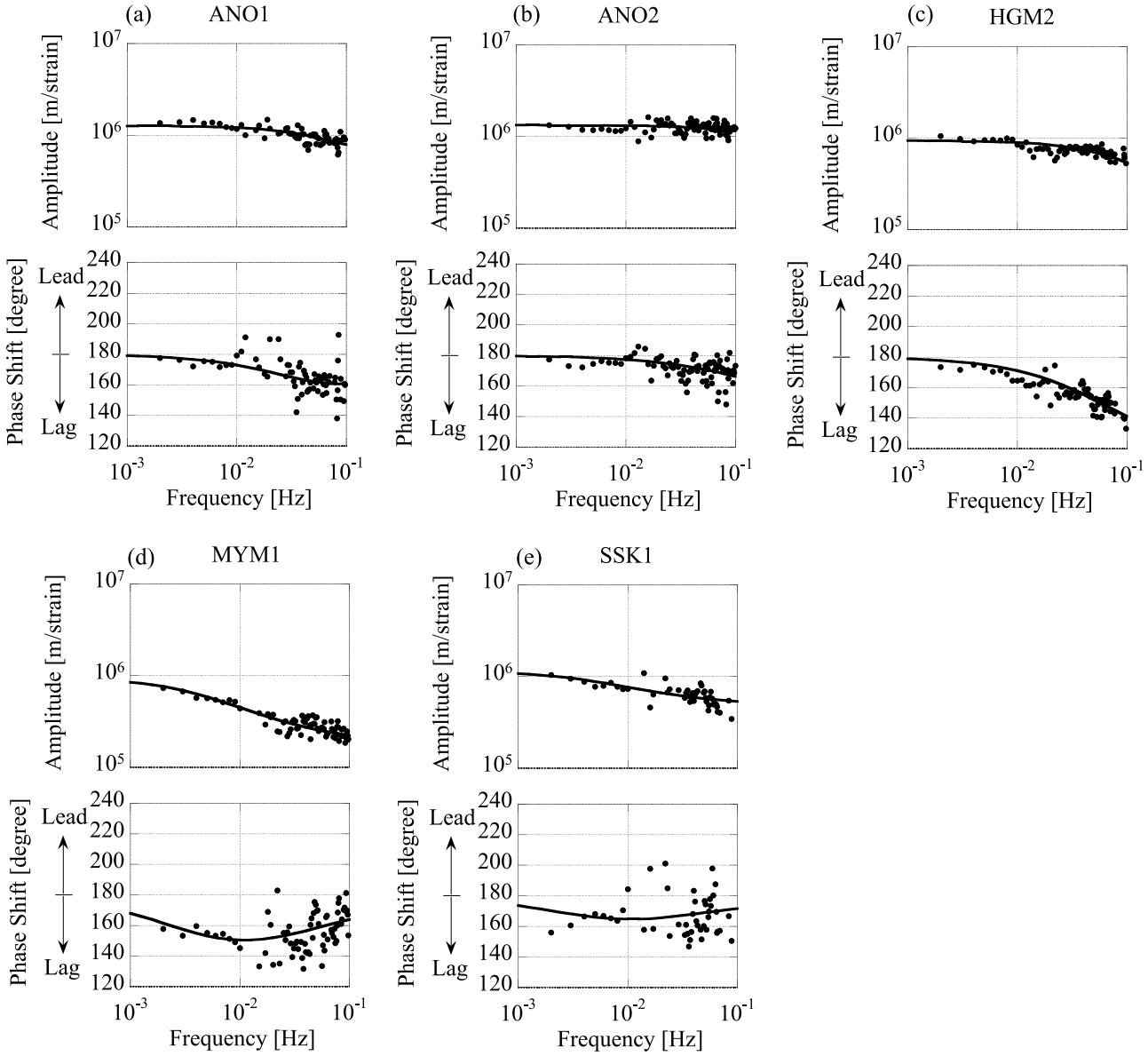

Figure 5. Amplitudes and phase shifts of the responses at (a) ANO1, (b) ANO2, (c) HGM2, (d) MYM1, and (e) SSK1. The solid circles indicate the values of the responses that are within a frequency range of 0.002 to 0.1 Hz and having a coherency larger than 0.8. The solid lines shows the solutions of equations (20) and (21) obtained using A_{vs} in Table 2 and T, S, K_uB/K_w, and A_w in Table 3.

and the water pressure in the well. The observed water pressure P_w in the well is sum of the water pressure $P_{\varepsilon kk}$ due to the elastic deformation of water and the water pressure P_Q due to the flow between the aquifer and the well.

$$P_w = P_{\varepsilon_{kk}} + P_Q. \tag{3}$$

The water pressure $P_{\varepsilon kk}$ due to the elastic deformation of water is expressed as

$$P_{\varepsilon_{kk}} = -K_w \frac{dV_w}{V_w} = -K_w A_w \varepsilon_{kk}, \tag{4}$$

where K_w is the bulk modulus of water, dV_w/V_w is the volumetric strain change of water in the well, ε_{kk} is volumetric strain change of the well-aquifer system, and A_w is the amplification factor of well volume change for ε_{kk}. The pore water pressure P_a in the aquifer is expressed as

$$P_a = -K_u B \varepsilon_{kk}, \tag{5}$$

where K_u is the undrained bulk modulus of the aquifer, B is the Skempton coefficient and the volumetric strain of the aquifer is supposed to be same as that of the well-aquifer system. The pressure change in the aquifer produces a flow between the aquifer and the well. The water pressure P_Q due to the flow is expressed as

$$\frac{dP_Q}{dt} = \frac{K_w Q}{V_w}, \tag{6}$$

where Q is the flow rate from the aquifer to the well.

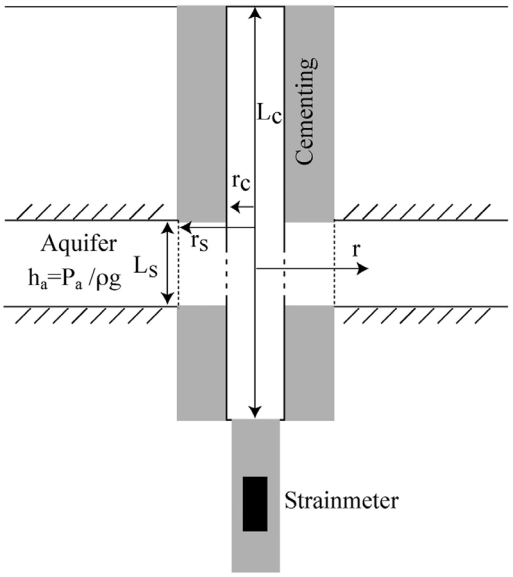

Figure 6. Idealized representation of a closed borehole well drilled into a confined aquifer and strainmeter.

[16] The flow between the aquifer and the well produces drawdown s (positive downward) of the head in the aquifer, which is expressed as the pressure-equivalent water column height. Based on *Hsieh et al.* [1987], in the absence of inertial effects, the water pressure oscillation in the well and the pore water pressure in the aquifer are related by

$$x = h_a - s_w, \tag{7}$$

where s_w is the drawdown at the well ($r = r_s$) due to Q, x is the head, i.e., the virtual water level in the well, and h_a is the head in the aquifer. Here, x and h_a, are obtained by dividing P_w and P_a by the density of water ρ and the acceleration of gravity g, respectively.

In radial coordinates, the equation governing water flow in the aquifer of the well-aquifer system is

$$\frac{\partial^2 s}{\partial r^2} + \frac{1}{r}\frac{\partial s}{\partial r} - \frac{S}{T}\frac{\partial s}{\partial t} = 0, \tag{8}$$

where T is the transmissivity of the aquifer, and S is the storage coefficient of the aquifer. This equation is the same as equation (A1) in Appendix A of *Hsieh et al.* [1987]. Solving for s of equation (8), we have

$$s_w = \frac{Q_0}{2\pi T}\{[\Phi Ker(\alpha_s) - \Psi Kei(\alpha_s)] + i[\Psi Ker(\alpha_s) + \Phi Kei(\alpha_s)]\} \cdot \exp(i\omega t), \tag{9}$$

where Q_0 is the complex amplitude of flow rate oscillation $Q = Q_0 \exp(i\omega t)$, ω is frequency of oscillation,

$$\Phi = \frac{-[Ker_1(\alpha_s) + Kei_1(\alpha_s)]}{2^{1/2}\alpha_s\left[Ker_1^2(\alpha_s) + Kei_1^2(\alpha_s)\right]}, \tag{10}$$

$$\Psi = \frac{-[Ker_1(\alpha_s) - Kei_1(\alpha_s)]}{2^{1/2}\alpha_s\left[Ker_1^2(\alpha_s) + Kei_1^2(\alpha_s)\right]} \tag{11}$$

and

$$\alpha_s = \left(\frac{\omega S}{T}\right)^{1/2} r_s, \tag{12}$$

where $Ker(\alpha_s)$ and $Kei(\alpha_s)$, and $Ker_1(\alpha_s)$ and $Kei_1(\alpha_s)$ are Kelvin functions of order 0 and 1, respectively [*Abramowitz and Stegun*, 1972].

Using equation (1), ε_{kk} and x can be expressed as

$$\varepsilon_{kk} = \frac{\varepsilon_{kk}^{obs}}{A_{vs}} = \frac{\varepsilon_0^{obs}}{A_{vs}}\exp(i\omega t) \tag{13}$$

and

$$x = x_0 \exp(i\omega t), \tag{14}$$

where ε_0^{obs} is the complex amplitude of the observed volumetric strain oscillation, and x_0 is the complex amplitude of virtual water level oscillation in the well.

Based on equations (3), (4), and (6), Q_0 is expressed as

$$Q_0 = i\omega V_w\left(\frac{\rho g x_0}{K_w} + \frac{A_w\varepsilon_0^{obs}}{A_{vs}}\right). \tag{15}$$

Based on equations (5) and (7), s_w is expressed as

$$s_w = -\left(x_0 + \frac{K_u B\varepsilon_0^{obs}}{\rho g A_{vs}}\right)\exp(i\omega t). \tag{16}$$

Based on equations (9), (15), and (16), the response of virtual water level x in the well to volumetric strain ε_{kk}^{obs} is expressed as

$$\frac{x_0}{\varepsilon_0^{obs}} = -\frac{1}{A_{vs}}\frac{K_w A_w}{\rho g}\frac{\frac{K_u B}{\rho g A_w}\frac{2\pi T}{\omega V_w} - A_2 + iA_1}{\frac{K_w}{\rho g}\frac{2\pi T}{\omega V_w} - A_2 + iA_1}, \tag{17}$$

where

$$A_1 = \Phi Ker(\alpha_s) - \Psi Kei(\alpha_s) \tag{18}$$

and

$$A_2 = \Psi Ker(\alpha_s) + \Phi Kei(\alpha_s). \tag{19}$$

The amplitude of equation (17) is expressed as

$$\left|\frac{x_0}{\varepsilon_0^{obs}}\right| = \frac{1}{A_{vs}}\frac{K_w A_w}{\rho g}\sqrt{\frac{\left(\frac{K_u B}{\rho g A_w}\frac{2\pi T}{\omega V_w} - A_2\right)^2 + A_1^2}{\left(\frac{K_w}{\rho g}\frac{2\pi T}{\omega V_w} - A_2\right)^2 + A_1^2}}, \tag{20}$$

and the phase shift of equation (17) is expressed as

$$\theta = a\tan 2\left(-\left(\frac{K_w}{\rho g} - \frac{K_u B}{\rho g A_w}\right)\frac{2\pi T}{\omega V_w}A_1, -\left\{\left(\frac{K_u B}{\rho g A_w}\frac{2\pi T}{\omega V_w} - A_2\right) \cdot \left(\frac{K_w}{\rho g}\frac{2\pi T}{\omega V_w} - A_2\right) + A_1^2\right\}\right). \tag{21}$$

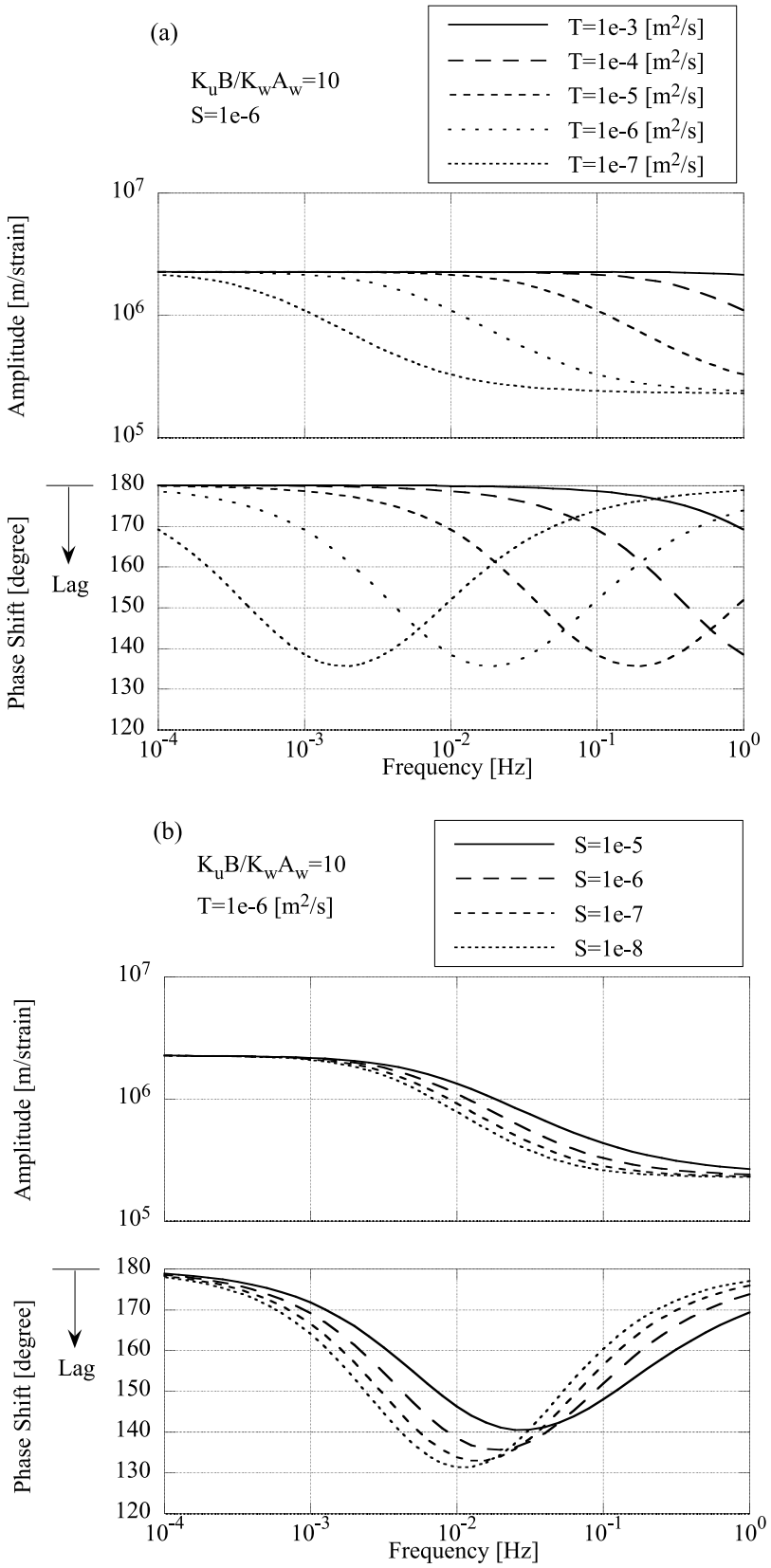

Figure 7. Plots of equations (20) and (21) for the case in which $K_uB/K_wA_w = 10$ for (a) S = 1e−6 and (b) T = 1e−6 (m^2/s). The curves are plotted in the frequency range of $\alpha_s \leq 2$.

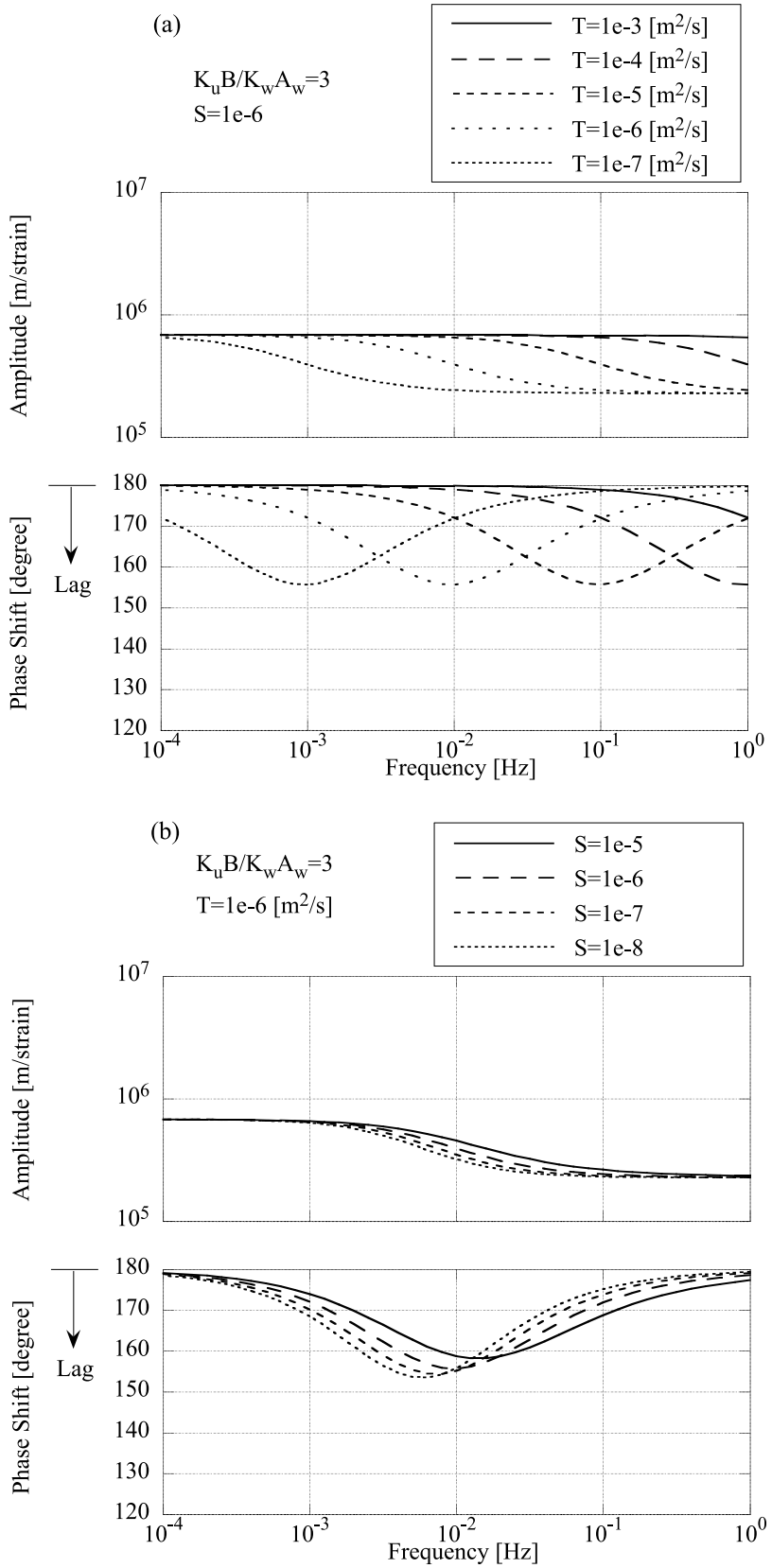

Figure 8. Plots of equations (20) and (21) for the case in which $K_uB/K_wA_w = 3$ for (a) $S = 1e - 6$ and (b) $T = 1e - 6$ (m^2/s). The curves are plotted in the frequency range of $\alpha_s \leq 2$.

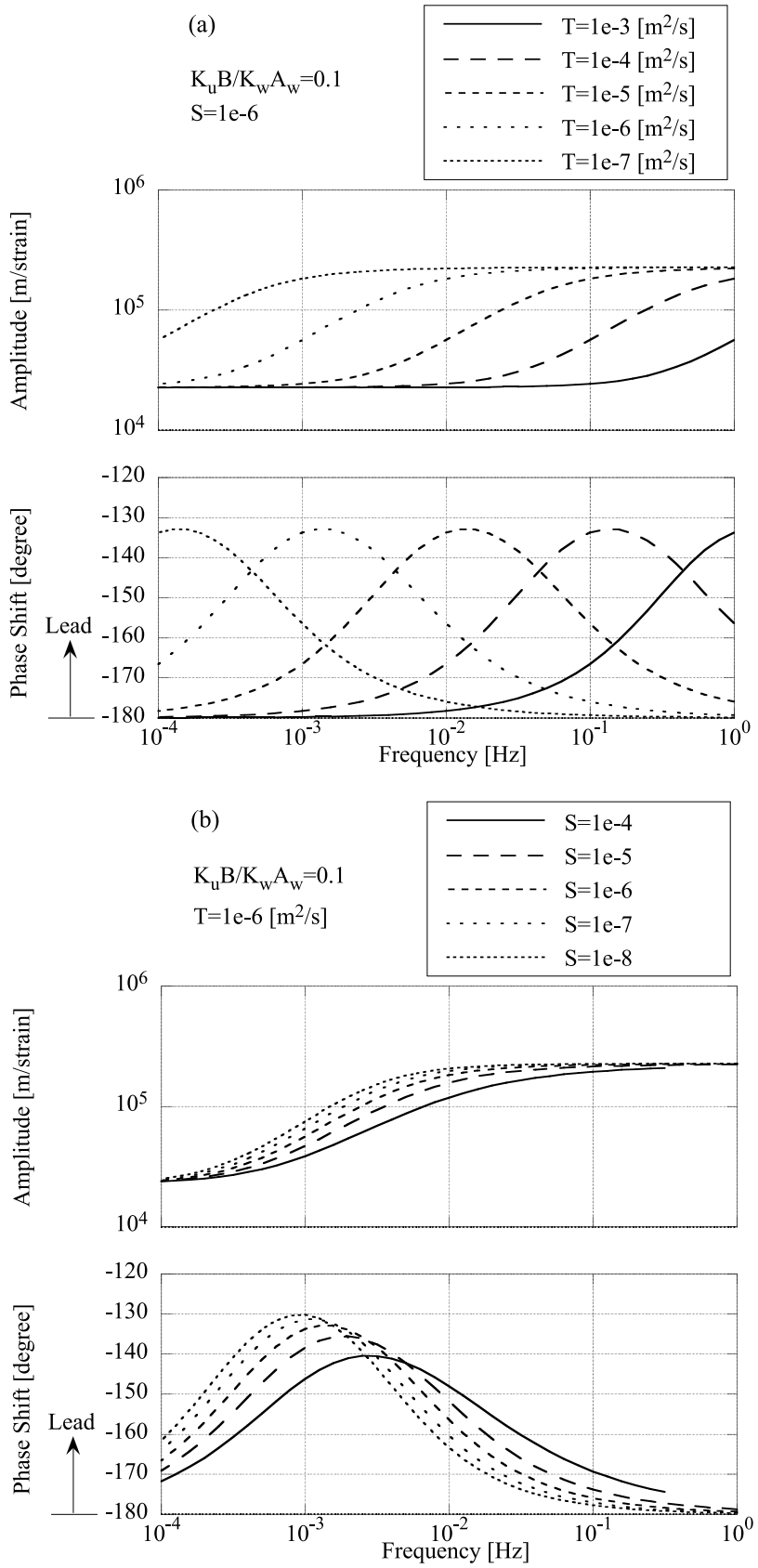

Figure 9. Plots of equations (20) and (21) for the case in which $K_uB/K_wA_w = 0.1$ for (a) S = 1e−6 and (b) T = 1e−6 (m^2/s). The curves are plotted in the frequency range of $\alpha_s \leq 2$.

Table 3. Properties of Aquifers at Five Closed Wells as Estimated From the Observed Responses

Station Code	Well Code	T (m^2/s)	S (dimensionless)	K_uB/K_w (1)	A_w (dimensionless)	$K_uB/\rho gA_{vs}$ (m/strain)	k (m^2)
ANO	ANO1	8e-6	4e-6	10.0	4.0	1.3e+6	5.5e-14
ANO	ANO2	1e-5	9e-5	10.5	0.5	1.3e+6	7.3e-14
HGM	HGM2	4e-6	5e-6	14.0	0.0	9.3e+5	1.9e-14
MYM	MYM1	5e-7	3e-5	14.0	2.5	9.3e+5	8.5e-16
SSK	SSK1	5e-7	9e-5	7.5	3.0	1.1e+6	1.2e-15

4.2. Characteristics of the Response

[17] In this section, values are calculated under the assumption that A_w and A_{vs} are 1. For the case in which $K_uB = K_wA_w$, the amplitude of response is $K_wA_w/\rho gA_{vs}$ with no phase shift, and the response has no frequency dependency. Here, K_w is approximately 2.2 GPa at 1 atm and 20°C, and so the amplitude of water pressure in the well is approximately 2.2 Pa per nanostrain, which is equivalent to 0.23 mm per nanostrain of the virtual water level, where ρ = 1,000 kg/m^3 and g = 9.8 m/s^2. When the volumetric strain is positive (dilatation), the water pressure is negative (decrease). Thus, the phase shift of the response is 180 degrees. In addition, the responses for the cases in which the aquifer is perfectly impermeable rock ($T = 0$) and the well has no screen are the same as that for the case in which $K_uB = K_wA_w$.

[18] For the case in which $K_uB \neq K_wA_w$, the amplitude of the response is approximately $K_uB/\rho gA_{vs}$ with no phase shift at low frequency ($\omega \rightarrow 0$), and is $K_wA_w/\rho gA_{vs}$ with no phase shift at high frequency ($\omega \rightarrow \infty$). In the intermediate range of frequency, the response exhibits frequency dependency. Figures 7, 8, and 9 show the amplitudes and phase shifts of the responses of a well-aquifer system in which L_c = 570 m, r_c = 0.075 m, L_s = 20 m, and r_s = 0.135 m, for various values of T, S, and K_uB/K_wA_w, by the approximate calculation in the frequency range of $\alpha_s \leq 2$. For the case in which $K_uB > K_wA_w$ (Figures 7 and 8), the amplitude decreases with increasing frequency. The phase lags at intermediate frequencies. For a significant portion of frequency band, the phase shift is more sensitive than the amplitude. For the case in which $K_uB < K_wA_w$ (Figure 9), the amplitude increases with increasing frequency. The phase leads at intermediate frequencies. With the exception of poorly consolidated sediments, the bulk modulus of rock and mineral is thought to be larger than that of water. Therefore, it is expected that there are very few deep and confined aquifers for which $K_uB < K_wA_w$. Note that T affects only the range in which the response exhibits frequency dependency, and S greatly affects the size of the phase shift, but only slightly affects the gradient of the amplitude and the range in which the response exhibits frequency dependency. In addition, K_uB/K_wA_w affects only the size of the amplitude and the phase shift and A_{vs} affects only the size of the amplitude.

[19] However, in the case that A_w is 0, the water pressure in equation (4) is zero. Therefore, the response at high frequency is different from the above mentioned response. The amplitude decays to zero and the phase largely lags at high frequency. The characteristics of the response are the same as *Hsieh et al.* [1987].

4.3. Comparison of the Expression With the Response Estimated From Data

[20] For T is in the range from 1e−9 to 9e−5, S is in the range from 1e−9 to 9e−5, K_uB/K_w is in the range from 1 to 20 at 0.5 interval and A_w is in the range from 0 to 10 at 0.5 interval, error sums of squares between the responses obtained from data and the expression are calculated. Table 3 shows the sets of parameter values, which minimize the error sum per one point in the case that there are 50 or more points (30 or more points at SSK1) in the frequency range of $\alpha_s \leq 2$. The solid curves in Figure 5 mean the solutions of equations (20) and (21) using the parameter values in Table 3. The average permeability k in the screened interval is defined as

$$k = T\mu/\rho gL_s, \tag{22}$$

where μ is the viscosity coefficient of water. μ is 1.002e−3 Pa s at 1 atm and 20°C. The values of permeability are listed in Table 3.

5. Discussion

[21] *Pickens et al.* [1987] discussed the problems associated with packer deformation for the case in which the water pressure is observed using the packer. The wells considered in the present paper are artesian wells and are closed by bolting a sealed iron cover onto the head of the well casing. Therefore, such problems are not encountered in the present study.

[22] The formulation in the present paper ignores the inertial effect, i.e., the kinetic energy of water. For the case in which the length and radius of the well are several hundred meters and tens of centimeters, respectively, the effect of water flow velocity is negligible for frequencies of less than 1 Hz. The higher-frequency phenomenon requires further validation. The correction of the difference in arrival times between the aquifer and the strainmeter for each phase of seismic waves may derive a more precise estimation of the response.

[23] Using the barometric responses of water pressure, whether the aquifer is confined is verified. The degree to which the aquifer is confined affects the frequency dependency of the long-period barometric response [e.g., *Quilty and Roeloffs*, 1991]. Figure 10 shows the barometric responses in the period ranging from 0.1 to 0.8 cycles per day. It is difficult to appropriately estimate the barometric response for long periods, because water pressure data contain long-term changes due to rainfall. At ANO1 and ANO2, the barometric responses are flat and so the aquifers are assumed to be very confined. At MYM1, the barometric response in the long-period range (>0.2 cycles per day) is not flat. This is believed to be an effect of rainfall or high-angle fractures in the rock. At HGM2 and SSK1, the amplitude of the barometric responses is not very flat. The reason for this may be that the dips of the fractures vary widely. At MYM1, HGM2, and SSK1, the phase shifts of

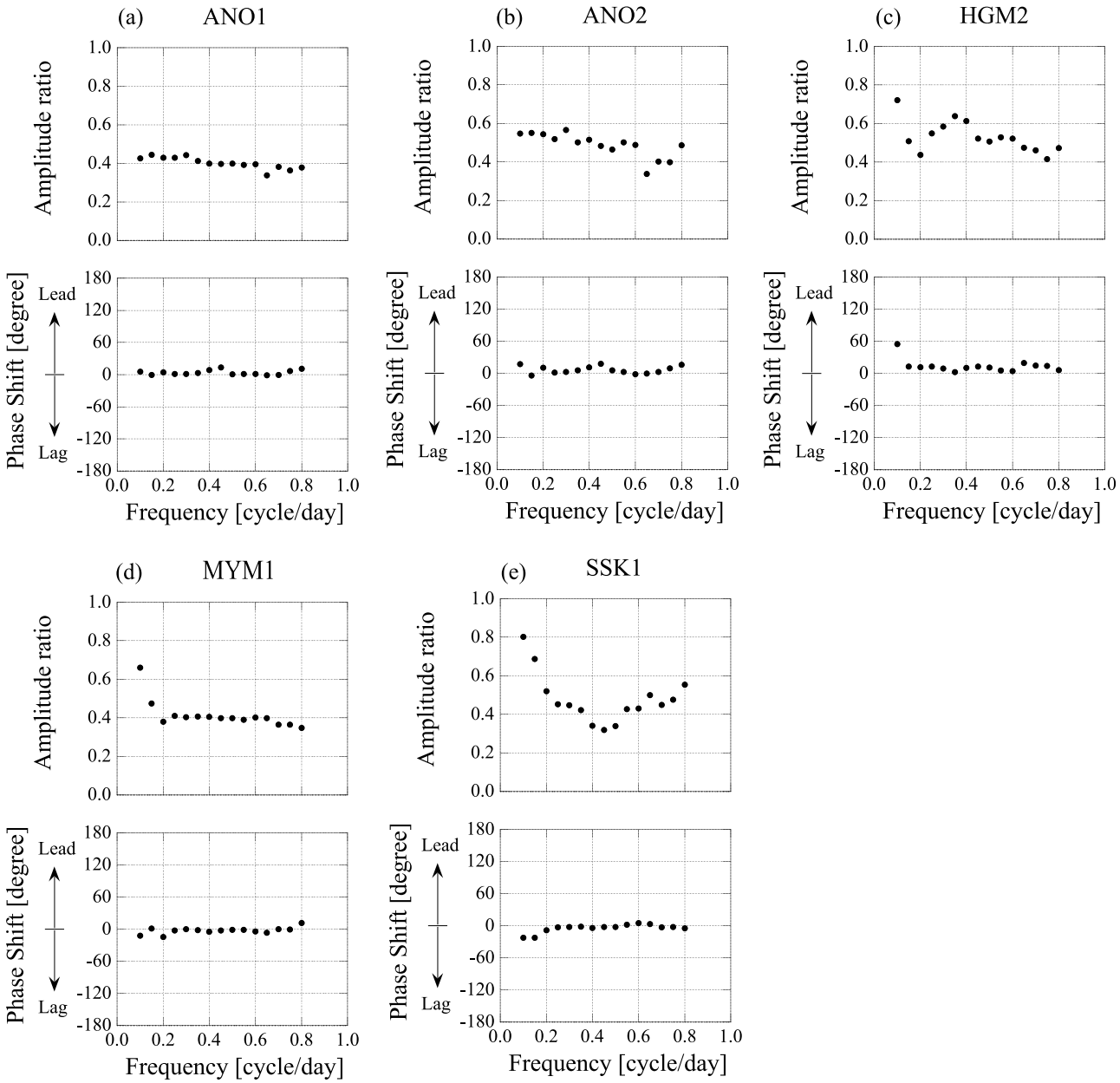

Figure 10. Amplitude ratios and phase shifts of the barometric responses at (a) ANO1, (b) ANO2, (c) HGM2, (d) MYM1, and (e) SSK1.

Table 4. Information of the Tidal Responses at the Five Closed Wells

Station Code	Well Code	Tidal Component	Period (h)	Amplitude (m/strain)	Error of Amplitude (m/strain)	Phase Shift (deg)	Error of Phase Shift (deg)
ANO	ANO1	O1	25.8	1.64e+6	1.24e+5	193.0	4.4
ANO	ANO1	M2	12.4	1.77e+6	3.01e+4	167.1	1.0
ANO	ANO2	O1	25.8	1.75e+6	2.67e+5	195.0	8.8
ANO	ANO2	M2	12.4	2.31e+6	6.69e+4	173.5	1.7
HGM	HGM2	O1	25.8	1.24e+6	1.35e+5	186.2	6.3
HGM	HGM2	M2	12.4	1.85e+6	5.22e+4	188.2	1.6
MYM	MYM1	O1	25.8	9.78e+5	2.93e+4	169.7	1.0
MYM	MYM1	M2	12.4	1.14e+6	7.17e+3	187.0	0.4
SSK	SSK1	O1	25.8	1.25e+6	2.00e+5	161.2	9.2
SSK	SSK1	M2	12.4	1.67e+6	4.05e+4	175.0	1.4

the barometric responses are flat, indicating that the aquifers are confined.

[24] Long-term data of water pressures in closed wells and crustal strains contain tidal components. Using the BAYTAP-G program [*Tamura et al.*, 1991], the tidal components are estimated from water pressure and crustal strain data. The response of water pressure to volumetric strain at each well was calculated (Table 4). For the case of a response under an undrained condition, the amplitude of the response is $K_uB/\rho gA_{vs}$. The amplitude of the tidal response at each well is slightly larger than that due to the seismic waves.

[25] The amplification factor A_w is described as follows. A_w are smaller than 1 at ANO2 and HGM2 whose depths are around 200 m. However, A_w are larger than 1 at ANO1, MYM1 and SSK1 whose depths were around 600 m. We suppose that A_w is caused by various physical properties around the well which is composed by a cylindrical iron casing, grout and surrounding rock (Figure 6). In particular, physical properties of the surrounding rock are essential for A_w because physical properties of the iron casing and grout are almost same in each well. It is a possible reason that rock in depth range of from 200 to 600 m tends to be harder than that in depth range of from 0 to 200 m.

[26] Besides depth-dependent characteristics of rock, vertical deformation of the well needs to be considered. It is difficult to estimate A_w by use of rock properties obtained in this paper. At present, there exists no method by which to independently estimate A_w. In the future, the value of A_w need be independently estimated in some manner. In addition, it is important to confirm whether two amplification factors A_w and A_{vs} exhibit frequency dependency. This may explain the difference between the tidal response and the response due to seismic waves.

6. Conclusions

[27] High-quality records of the oscillations of water pressures in closed wells and crustal strains due to the seismic waves of the 2010 Chile earthquake were obtained. The oscillations of water pressures were compared with the oscillations of crustal strains, and the frequency characteristics of the responses of water pressures in closed wells were then estimated. An expression for the response of water pressure in a closed well to crustal strain was developed. Except for the case that A_w is 0, the response at high-frequency limit has constant amplitude with no phase shift, due to the elastic deformation of water. It is different from the response in an open well. On the other hand, the response at low frequency is the same as the response in an open well. This expression explains the frequency characteristics of the responses estimated from water pressure and crustal strain data. This response is useful for the estimation of rock properties.

[28] **Acknowledgment.** We thank reviewers Chi-Yuen Wang, Earl Davis, and Tomochika Tokunaga for pointing out a few errors in the mathematical solutions presented in the manuscript and the Associate Editor Kelin Wang for his suggestion to introduce parameter Aw into equation (4) to fix an error. We are grateful to Osamu Kamigaichi for providing the program to calculate the synthetic seismogram of strain from source solution of the earthquake.

References

Abramowitz, M., and I. A. Stegun (Eds.) (1972), *Handbook of Mathematical Functions, Applied Mathematics*, Natl. Bur. of Stand., Washington, D. C.

Cooper, H. H., Jr., J. D. Bredehoeft, I. S. Papadopulos, and R. R. Bennett (1965), The response of well-aquifer systems to seismic wave, *J. Geophys. Res.*, *70*, 3915–3926, doi:10.1029/JZ070i016p03915.

Dziewonski, A. M., T.-A. Chou, and J. H. Woodhouse (1981), Determination of earthquake source parameters from waveform data for studies of global and regional seismicity, *J. Geophys. Res.*, *86*, 2825–2852, doi:10.1029/JB086iB04p02825.

Hsieh, P. A., J. D. Bredehoeft, and J. M. Farr (1987), Determination of aquifer transmissivity from Earth tide analysis, *Water Resour. Res.*, *23*, 1824–1832, doi:10.1029/WR023i010p01824.

Ishii, H., T. Yamauchi, S. Matsumoto, Y. Hirata, and S. Nakao (2002), Development of multi-component borehole instrument for earthquake prediction study: Some observed examples of precursory and co-seismic phenomena relating to earthquake swarms and application of the instrument for rock mechanics, in *Seismogenic Process Monitoring*, edited by H. Ogasawara, T. Yanagidani, and M. Ando, pp. 365–377, A. A. Balkema, Lisse, Netherlands.

Kano, Y., and T. Yanagidani (2006), Broadband hydroseismograms observed by closed borehole wells in the Kamioka mine, central Japan: Response of pore pressure to seismic waves from 0.05 to 2 Hz, *J. Geophys. Res.*, *111*, B03410, doi:10.1029/2005JB003656.

Kitagawa, Y., N. Koizumi, M. Takahashi, N. Matsumoto, and T. Sato (2006), Changes in groundwater levels or pressures associated with 2004 off the west coast of northern Sumatra earthquake (M9.0), *Earth Planets Space*, *58*, 173–179.

Lay, T., C. J. Ammon, H. Kanamori, K. D. Koper, O. Sufri, and A. R. Hutko (2010), Teleseismic inversion for rupture process of the 27 February 2010 Chile (M_w 8.8) earthquake, *Geophys. Res. Lett.*, *37*, L13301, doi:10.1029/2010GL043379.

Liu, L.-B., E. Roeloffs, and X.-Y. Zheng (1989), Seismically induced water level fluctuations in the Wali Well, Beijing, China, *J. Geophys. Res.*, *94*, 9453–9462, doi:10.1029/JB094iB07p09453.

Pickens, J. F., G. E. Grisak, J. D. Avis, D. W. Belanger, and M. Thury (1987), Analysis and interpretation of borehole hydraulic tests in deep boreholes: Principles, model development, and applications, *Water Resour. Res.*, *23*, 1341–1375, doi:10.1029/WR023i007p01341.

Quilty, E. G., and E. A. Roeloffs (1991), Removal of barometric pressure response from water level data, *J. Geophys. Res.*, *96*, 10,209–10,218, doi:10.1029/91JB00429.

Roeloffs, E. A. (1996), Poroelastic techniques in the study of earthquake-related hydrologic phenomena, *Adv. Geophys.*, *37*, 135–195, doi:10.1016/S0065-2687(08)60270-8.

Rojstaczer, S. (1988), Determination of fluid flow properties from the response of water levels in wells to atmospheric loading, *Water Resour. Res.*, *24*, 1927–1938, doi:10.1029/WR024i011p01927.

Tamura, Y., T. Sato, M. Ooe, and M. Ishiguro (1991), A procedure for tidal analysis with a Bayesian information criterion, *Geophys. J. Int.*, *104*, 507–516, doi:10.1111/j.1365-246X.1991.tb05697.x.

Wang, H. F. (2000), *Theory of Linear Poroelasticity With Applications to Geomechanics and Hydrogeology*, 287 pp., Princeton Univ. Press, Princeton, N. J.

S. Itaba, Y. Kitagawa, N. Koizumi, and N. Matsumoto, Active Fault and Earthquake Research Center, Geological Survey of Japan, National Institute of Advanced Industrial Science and Technology, Site C7, 1-1-1 Higashi, Tsukuba, Ibaraki 305-8567, Japan. (y-kitagawa@aist.go.jp)